Fe XIV green/Fe XIII infrared line ratio diagnostics

A. K. Srivastava[1,*], Jagdev Singh[2], B. N. Dwivedi[1], S. Muneer[2],
T. Sakurai[3] and K. Ichimoto[3]

[1] *Department of Applied Physics, Institute of Technology, Banaras Hindu University, Varanasi 221 005, India*
[2] *Indian Institute of Astrophysics, Bangalore 560 034, India*
[3] *National Astronomical Observatory, Osawa, Mitaka, Tokyo, Japan*

Abstract. We consider the first 27-level atomic model of Fe XIII (5.9 K < $\log T_e$ < 6.4 K) to estimate its ground level populations, taking account of electron as well as proton collisional excitations and de-excitations, radiative cascades, radiative excitations and de-excitations. Radiative cascade is important but the effect of dilution factor is negligible at higher electron densities. The ${}^3P_1$-${}^3P_0$ and ${}^3P_2$-${}^3P_1$ transitions in the ground configuration $3s^2\,3p^2$ of Fe XIII result in two forbidden coronal emission lines in the infrared region, namely 10747 and 10798 Å. While the 5303 Å green line is formed in the $3s^2$ 3p ground configuration of Fe XIV as a ${}^2P_{3/2}$-${}^2P_{1/2}$ magnetic dipole transition. The line-widths of simultaneously observed Fe XIV green and Fe XIII infrared forbidden coronal emission lines can be a useful diagnostic tool to deduce temperature and nonthermal velocity in the largescale coronal structures using intensity ratios of the lines as the temperature signature, instead of assuming ion temperature to be equal to the electron temperature. Since the line intensity ratios $I_{G5303}/I_{IR10747}$ and $I_{G5303}/I_{IR10798}$ have very weak density dependence, they are ideal monitors of temperature mapping in the solar corona. The computed ratios will be compared with the recently obtained observations in our next paper.
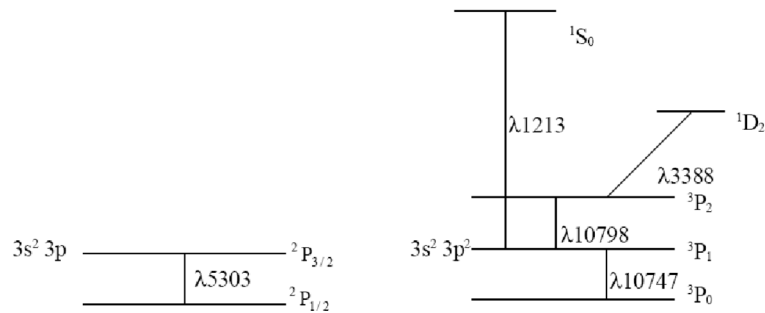
Keywords : Sun : corona – Sun : infrared

---

*Present address: Armagh Observatory, College Hill, Armagh, Northern Ireland BT61 9DG.

1. Introduction

The density diagnostic efficiency of the line intensity ratio $I_{IR10747}/I_{IR10798}$, has been explored since the works of Dumont & Perche (1964), Chevalier & Lambert (1969), Zirker (1970), de Boer, Olthof & Pottasch (1972), Flower & des Forêts (1973). These two forbidden coronal emission lines of Fe XIII lie in the infrared region of the electromagnetic spectrum. The 5303 Å green line of Fe XIV has also been important since the pioneering work of Edlén (1942) and indicates the million degree temperature of the solar corona. Schematic representation of formations of Fe XIV green line and Fe XIII infrared lines are given in Fig. 1.

The $^3P_1$ level of Fe XIII 10747 Å line is collisionally excited from the $^3P_0$ level mainly by photospheric radiation, but at higher densities cascade effect from upper levels becomes important. In the formation of 10798 Å lines, $^3P_2$ level is collisionally excited from the $^3P_0$ level and cascade effect from the upper levels. Flower & des Forêts (1973) have shown the dominance of indirect excitations by considering 27-level atomic model for Fe XIII. They have considered the electron as well as proton collisional excitations and radiative excitation as direct processes for excitation of the first five levels and dominant radiative cascades from the upper levels into these ground term levels namely $3s^23p^2$ $^1S_0$, $3s^23p^2$ $^1D_2$ and $3s^23p^2$ $^3P_{2,1,0}$. Upper levels are also populated by collisions. In this paper we have considered the 27-level model and recently reported atomic data by Young (2004) and Aggarwal & Keenan (2004, 2005), for the wide temperature range 5.9 K$<$log $T_e$$<$6.4 K and for density of 10^9 cm^{-3}. This is the mean density of our range of interest 1×10^8 cm^{-3} $<$Ne$< 1 \times 10^{10}$ cm^{-3}. Dilution factor has no appreciable effect on the infrared lines at higher densities and it is taken to be 0.3 for the given coronal conditions. The Fe XIV 5303 Å green coronal emission line, is formed by taking both radiative and collisional processes. We have taken the Mason's (1975) excitation calculations for the emissivity of the green line in the inner corona. Ionization equilibrium calculations are taken from Arnaud & Rothenflug (1985).

Figure 1. Fe XIV and Fe XIII coronal lines for plasma diagnostics.

In this paper, we report the line Intensity ratio of $I_{G5303}/I_{IR10747}$ and $I_{G5303}/I_{IR10798}$. We have followed the same approach as of Orrall et al. (1990). Assuming coronal gas in radial hydrostatic equilibrium along the line of sight, intensity ratios are reported for a wide temperature range 5.9 K < log T_e < 6.4 K. In section 2 we present the statistical equilibrium equations and line emissivity. Section 3 deals with Fe XIV green/Fe XIII infrared theoretical line ratios. Results and discussion are given in the last section.

2. Statistical equilibrium equations and line emissivity

We have solved the statistical equilibrium equations for the first five levels of the ground state configuration 3s^2 3p^2 of Fe XIII. Electron as well as proton collisional excitations along with the radiative excitations are considered as direct excitation mechanisms. The radiative cascades from twenty two fine-structured levels of two consecutive excited configurations 3s 3p^3 and 3s^2 3p 3d, are considered as a significant indirect process for the determination of level populations of the first five levels in ground state configuration 3s^2 3p^2.

The statistical equilibrium equations are given as (cf., Flower & des Forêts 1973).

$$\sum_{j=1}^{m} d_{ij} N_j = 0 \tag{1}$$

with d_{ij} is defined as

$$d_{ji} = A'_{ij} + N_e \left\{ q_{ij} + 0.8 r_{ij} + \sum_{k=m+1}^{n} q_{ik} c_{kj} \right\} \tag{2}$$

for $i \neq j$,

$$d_{ii} = -\sum_{j \neq i} d_{ji}, \tag{3}$$

and

$$\sum_{j=1}^{m} N_j = N, \tag{4}$$

where N is the total ion density. The first term on the right in equation (2) represents the probability of a radiative transition $(i \rightarrow j)$ which is given by

$$A'_{ij} = \left\{ \begin{array}{ll} W \frac{\omega_j}{\omega_i} \frac{A_{ji}}{e^{\Delta E_{ij}/kT_r} - 1} & \text{for} \quad j > i \\ A_{ij} + \frac{\omega_j}{\omega_i} A'_{ji} & \text{for} \quad i > j \end{array} \right\} \tag{5}$$

where T_r is the temperature of incident photospheric radiation which is equal to 6000 K.

A_{ji} is the probability of spontaneous radiative transition $(j \rightarrow i)$. q_{ij} is electron collision rate coefficient and is defined by

$$q_{ij} = 8.63 \times 10^{-6} \frac{\gamma_{ij}}{\omega_i T_e^{1/2}} \tag{6}$$

where

$$\gamma_{ij} = \left\{ \begin{array}{lll} \Omega_{ij} e^{-\Delta E_{ij}/kT_e} & \text{for} & j > i \\ \Omega_{ij} & \text{for} & i > j \end{array} \right\}. \tag{7}$$

It is also reasonable to assume the Maxwellian velocity distribution at the same kinetic temperature for protons and electrons.

We have adopted the energy level model of the first twenty seven levels of Fe XIII and relevant collision strengths from Aggarwal & Keenan (2004, 2005). Values of spontaneous radiative transition probabilities are taken from Young (2004). We have used the ionization equilibrium and cascade rate coefficients of Arnanud & Rothenflug (1985) and Flower and des Forêts (1973) respectively. We have solved the statistical equlibrium equation using the matrix inversion method to find the relative level populations of ground term levels.

The emissivity of infrared lines of Fe XIII is given by

$$E(\lambda_{ij}) = N_j(\text{Fe XIII})A_{ji}\frac{hc}{\lambda_{ij}}, \text{ ergs cm}^{-3}\text{ s}^{-1}(j > i) \tag{8}$$

where N_j (Fe XIII) is number density of the upper level which can be parameterized as,

$$N_j(\text{Fe XIII}) = \frac{N_j(\text{Fe XIII})}{N(\text{Fe XIII})} \cdot \frac{N(\text{Fe XIII})}{N(\text{Fe})} \cdot \frac{N(\text{Fe})}{N(\text{H})} \cdot \frac{N(\text{H})}{N_e} \cdot N_e \tag{9}$$

where $\frac{N_j(\text{Fe XIII})}{N(\text{Fe XIII})}$ is the relative level population of the upper level j, N (Fe XIII)/N(Fe) is the relative ionic fraction in ionization equilibrium, $\frac{N(\text{Fe})}{N(\text{H})}$ is relative element abundance 7×10^{-5} (Mason 1975) and for a fully ionized plasma $\frac{N(H)}{N_e} \approx 0.8$.

3.   Fe XIII and Fe XIV line intensity ratios

Line intensity observed at a height x above the limb can be written as (cf., Orrall et al. 1990; Guhathakurta et al. 1992)

$$I_j(x) = R_o \left(\frac{2\pi h_0}{\gamma_i}\right)^{1/2} x^{3/2} E_i(x_0) \exp\left[-\frac{\gamma_i(x - x_0)}{h_0 x x_0}\right] \tag{10}$$

where h_0 is the scale height and x_0 is the reference height.

In the inner corona, the emissivity E_i of a forbidden line is approximated as

$$E_i = D_i(T)N_e^{\gamma_i} \text{ ergs cm}^{-3} \text{ s}^{-1} \text{ sr}^{-1} \qquad (11)$$

where $i = IR10747$ and $i = IR10798$ for the two infrared lines of Fe XIII and i = G5303 for the green line of Fe XIV. $D_i(T)$ is theoretical emissivity which depends on temperature, atomic parameters and radiation field as well as the elemental abundance. The power of electron density N_e lies between $1 < \gamma < 2$ for the forbidden lines (Dwivedi 1993). Using the calculated Fe XIII emissivities at its formation temperature, we find $\gamma = 1.77$ for the line 10747 Å and $\gamma = 1.67$ for 10798 Å line. For Fe XIV 5303 Å line we have adopted the value $\gamma = 1.68$ from Guhathakurtha (1992, 1993). Using equation (10) and solving the following equations,

$$D_{IR10747}(T) = \frac{E_{IR10747}}{N_e^{1.77}}, \qquad (12a)$$

$$D_{IR10798}(T) = \frac{E_{IR10798}}{N_e^{1.67}}, \qquad (12b)$$

and

$$D_{G5303}(T) = \frac{E_{G5303}}{N_e^{1.68}}, \qquad (12c)$$

we obtain

$$\frac{I_{G5303}}{I_{IR10747}} = 1.0265(\frac{D_{G5303}(T)}{D_{IR10747}(T)}) \cdot N_e^{-0.09}, \qquad (13)$$

and

$$\frac{I_{G5303}}{I_{IR10798}} = 0.9970(\frac{D_{G5303}(T)}{D_{IR10798}(T)}) \cdot N_e^{0.01}. \qquad (14)$$

These line intensity ratios have very weak density dependence, however, they strongly depend on temperature.
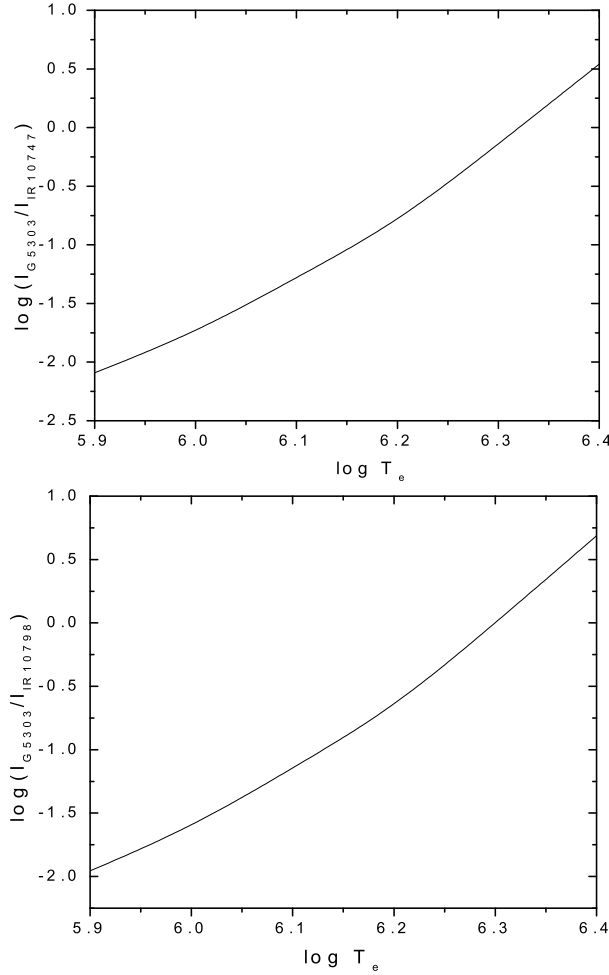
The intensity ratios given by equations (13) and (14) are shown in Figure 2. We also find the best fit for the intensity ratios in the form of second order polynomial fit:

$$\log(I_{G5303}/I_{IR10747}) = [135.10736 - 49.55222(\log T_e) + 4.45734(\log T_e)^2] \qquad (15a)$$

and

$$\log(I_{G5303}/I_{IR10798}) = [137.85857 - 50.42675(\log T_e) + 4.5304(\log T_e)^2] \qquad (15b)$$

The equations (15a) and (15b) are only valid for the given temperature range of 5.9 K < $\log T_e < 6.4$ K.

Figure 2. Temperature-dependence of the theoretical line intensity ratio $I_{G5303}/I_{IR10747}$ and $I_{G5303}/I_{IR10798}$.

4.   Results and discussion

These line intensity ratios are almost density independent. The theoretical line ratios $I_{G5303}/I_{IR10747}$ and $I_{G5303}/I_{IR10798}$ show the increasing pattern with enhancement temperature and are useful for determining the temperature structure along the loop length. Non-thermal velocities can be calculated by using FWHM of observed lines, using the computed temperature by these intensity ratios. This is not the temperature of maximum abundances. The temperature and nonthermal velocity inside the coronal structures can be correlated as $\frac{2kT}{M} + \xi^2 = \left(\frac{1}{4\ln 2}\right) c^2 \,(\text{FWHM}/\lambda)^2$, where T is the kinetic temperature, k

is the Boltzman constant, m is the ion mass, ξ is the nonthermal velocity, c is the velocity of light, λ is wavelength, and FWHM is the full-width half-maximum of the observed lines.

The theoretical line intensity ratios are double valued function of the temperature, hence, indicate the existence of the plasma of different temperatures at the same height. Our present theoretical study provides temperature dependent line ratios, which are useful in the mapping of temperature and nonthermal velocity in coronal structures. Temperature and nonthermal velocity are very crucial in the study of wave activity in these long-lived coronal structures. This theoretical work has been done in view of recently obtained simultaneous raster scans of coronal loops in these emission lines using 25 cm coronagraph of Norikura observatory of NAOJ, Japan. The computed ratios will be compared with the observations in our next paper, and will yield temperature and nonthermal velocity map. This paper provides description about the theoretical part of our work. Our computational programmes will use the theoretically calculated parameters and observational data to map the coronal temperature and nonthermal velocity. These measurements will be useful to explore the exact trend of the variation of turbulence and wave activity in coronal loops.

Acknowledgements

References

Aggarwal, K.M., & Keenan, F.P., 2004, A&A, 418, 371

Aggarwal, K.M., & Keenan, F.P., 2005, A&A, 429, 1117

Arnaud, M., & Rothenflug, R., 1985, A&AS, 60, 425

Chevalier, R.A., & Lambert, D.L., 1969, SoPh, 10, 115

de Boer, K.S., Olthof, H., & Pottasch, S.R., 1972, A&A, 16, 417

Dumont, J.P., & Perche, J.C., 1964, Mém. Soc. R. Sci. Liége, 9, 186

Dwivedi, B.N., 1993, SSRv, 65, 289

Edlen, B., 1942, ZA, 22, 30

Flower, D.R., & des Forêts, G.P., 1973, A&A, 24, 181

Guhathakurta, M., Rottman, G.J., Fisher, R.R., Orrall, F.Q., & Altrock, R.C., 1992, ApJ, 388, 633

Guhathakurta, M., Fisher, R.R., & Altrock, R.C., 1993, ApJ, 414, 145

Mason, H.E., 1975, MNRAS, 170, 651

Orrall, F.Q., Rottmann, G.J., Fisher, R.R., & Munro, R.H., 1990, ApJ., 349, 656

Young, P.R., 2004, A&A, 417, 785

Zirker, J.B., 1970, SoPh, 11, 68